



ELSEVIER



# Cranial bone structure in children with sagittal craniosynostosis: Relationship with surgical outcomes<sup>☆</sup>

Naiara Rodriguez-Florez<sup>a,b,\*</sup>, Amel Ibrahim<sup>a,b</sup>,  
J. Ciaran Hutchinson<sup>a,b</sup>, Alessandro Borghi<sup>a,b</sup>, Greg James<sup>a,b</sup>,  
Owen J. Arthurs<sup>a,b</sup>, Patrizia Ferretti<sup>a</sup>, David Dunaway<sup>a,b</sup>,  
Silvia Schievano<sup>a,b,c</sup>, N. U. Owase Jeelani<sup>a,b</sup>

<sup>a</sup> UCL Great Ormond Street Institute of Child Health, London, UK

<sup>b</sup> Great Ormond Street Hospital for Children NHS Foundation Trust, London, UK

<sup>c</sup> UCL Institute of Cardiovascular Science, Centre for Cardiovascular Imaging, London, UK

Received 30 November 2016; accepted 18 June 2017

## KEYWORDS

Cranial bone;  
Craniosynostosis;  
Spring-assisted  
cranioplasty;  
Micro-CT;  
3D scanning

**Summary** *Background:* While spring-assisted cranioplasty has become a widespread technique to correct scaphocephaly in children with sagittal synostosis, predicting head shape changes induced by the gradual opening of the springs remains challenging. This study aimed to explore the role of cranial bone structure on surgical outcomes.

*Methods:* Patients with isolated sagittal synostosis undergoing spring-assisted cranioplasty at GOSH (London, UK) were recruited ( $n = 18$ , age: 3–8 months). Surgical outcome was assessed by the change in cephalic index measured on 3D head scans acquired before spring insertion and after their removal using a 3D handheld scanner. Parietal bone samples routinely discarded during spring-assisted cranioplasty were collected and scanned using micro-computed tomography. From visual assessment of such scans, bone structure was classified into one- or three-layered, the latter indicating the existence of a diploë cavity. Bone average thickness, volume fraction and surface density were computed and correlated with changes in cephalic index.

*Results:* Cephalic index increased for all patients ( $p < 0.001$ ), but individual improvement varied. Although the patient age and treatment duration were not significantly correlated with changes in cephalic index, bone structural parameters were. The increase of cephalic index was smaller with increasing bone thickness (Pearson's  $r = -0.79$ ,  $p < 0.001$ ) and decreasing bone surface density ( $r = 0.77$ ,  $p < 0.001$ ), associated with the three-layered bone structure.

<sup>☆</sup> This work was presented at 1) *European Association of Plastic Surgeons (EURAPS)* meeting in May 26–28, 2016 in Brussels (Belgium) and at 2) *European Society of Biomechanics (ESB)* conference in July 10–13, 2016 in Lyon (France).

\* Corresponding author. SCRUM Section, Room 160, Developmental Biology and Cancer Programme, UCL Great Ormond Street Institute of Child Health, 30 Guilford Street, London WC1N 1EH, UK.

E-mail address: [n.florez@ucl.ac.uk](mailto:n.florez@ucl.ac.uk) (N. Rodriguez-Florez).

**Conclusions:** Variation in parietal bone micro-structure was associated with the magnitude of head shape changes induced by spring-assisted cranioplasty. This suggests that bone structure analysis could be a valuable adjunct in designing surgical strategies that yield optimal patient-specific outcomes.

© 2017 British Association of Plastic, Reconstructive and Aesthetic Surgeons. Published by Elsevier Ltd. This is an open access article under the CC BY license (<http://creativecommons.org/licenses/by/4.0/>).

## Introduction

Spring-assisted cranioplasty (SAC) has become an increasingly widespread technique to correct scaphocephaly in young infants with sagittal craniosynostosis.<sup>1–7</sup> SAC involves the fashioning of sagittal or parasagittal osteotomies and the temporary placement of spring-like metallic distractors, which affect an ongoing intra- and post-operative expansion to widen the biparietal width of the skull. Overall, skull remodelling occurs in the subsequent weeks and months,<sup>8</sup> and the springs are removed after approximately 4 months.

The most common way of assessing surgical outcome in SAC is by measuring the cephalic index (CI), defined as the ratio between cranial width and length.<sup>1,3,6,8,9</sup> After spring removal, a 'good' surgical outcome is characterised by a shorter and wider head shape compared to pre-operative shape, which is reflected in an increase in CI. One of the differences of SAC over other techniques is that the overall change in head shape is not immediate but happens over time. As such, at present, it is unclear which patient and operative factors influence the final change in the CI. Understanding these factors will allow surgeons to make decisions about optimal techniques for individual children.

One of the factors that is known to favour larger changes in CI is the age of the patient, with younger patients found to benefit more from SAC, presumably because of their skull being more malleable.<sup>1,4,7,9</sup> However, in our experience, age alone is not always an accurate predictor of the change in CI with SAC.

Considering that springs work by exerting force on adjacent cranial bone, bone structure is expected to influence the response of the cranium to this mechanical treatment,<sup>10–12</sup> thus affecting head shape.<sup>13–15</sup> The cranial bone grows through intramembranous ossification, evolving from a one-layered cancellous tissue that easily adapts to the growing brain, to a complex sandwich-like three-layered structure that is ideal to absorb impacts.<sup>16–18</sup> This sandwich structure is composed of inner and outer layers of compact bone (termed 'tables') and spongy tissue called 'diploë' in between. Although the micro-structural differences have implications in the mechanics, it is not clear at which exact stage during development this one- to three-layer transition happens.<sup>17</sup>

The current study aimed to investigate the micro-structure of the cranial bone in infants with sagittal craniosynostosis undergoing SAC to better understand the impact of the cranial bone on surgical outcomes. Bone structural properties were derived from high-resolution micro-computed tomography, while surgical outcomes

were assessed by measuring the CI on 3D head scans acquired using a 3D handheld scanner.

## Methods

### Patient population

Eighteen consecutively consented patients with non-syndromic, single suture, sagittal synostosis (1 female, 17 males) who underwent SAC at Great Ormond Street Hospital for Children (GOSH, London, UK) were prospectively recruited for this study between May 2015 and February 2016. The age of the patients at the time of spring insertion was  $5.3 \pm 1.1$  months, and springs were removed  $4.2 \pm 0.8$  months later (Table 1). Written parental consent was obtained in the pre-operative clinic for bone collection and head 3D scanning. Tissue samples were collected under ethical approval from the Camden and Islington Community Local Research Ethics Committee (London, UK). All bone samples were handled in accordance with the Human Tissue Act requirements.

**Table 1** Details of the recruited patients with sagittal synostosis, including gender, age at spring insertion and removal, and duration between spring insertion and removal.

	Gender	Age at insertion (months)	Age at removal (months)	Time from insertion to removal (months)
P1	Male	3.7	8.1	4.4
P2	Male	4.1	8.7	4.6
P3	Male	4.1	9.7	5.6
P4	Male	4.3	8.6	4.3
P5	Male	4.7	7.9	3.2
P6	Male	4.8	7.9	3.1
P7	Male	4.8	10.0	5.2
P8	Male	4.9	9.3	4.4
P9	Male	5.0	10.2	5.2
P10	Male	5.4	9.4	4.0
P11	Male	5.4	9.0	3.6
P12	Male	5.5	8.9	3.4
P13	Male	5.6	8.7	3.1
P14	Male	5.7	9.2	3.5
P15	Male	6.1	10.7	4.6
P16	Male	7.2	11.9	4.7
P17	Male	7.2	11.4	4.2
P18	Female	7.4	11.6	4.2

## SAC surgical technique

SAC is performed at GOSH to correct scaphocephaly in young children with sagittal synostosis. Details about the surgical technique can be found at Rodgers et al. (2017).<sup>19</sup> Spring insertion is performed with the patient in prone position through one small transverse scalp incision. After making a rectangular craniotomy around mid-way between the coronal and lambdoid sutures, two parasagittal osteotomies are made extending from the coronal to lambdoid sutures. Two standardised metal springs (Active Spring Company, Thaxted, UK) are then placed on each side of the osteotomy. The springs open gradually, driving the skull to widen on-table and over subsequent weeks and months. Approximately 4–5 months after insertion, the springs are removed with a second short procedure.

## Bone collection and analysis

Rectangular bone samples, containing left and right parietal bone and fused sagittal suture, usually discarded when performing the craniotomy during SAC (Figure 1) were collected from the operation theatre in a sterile Falcon tube containing Leibovitz's L-15 media (Gibco) ( $n = 18$ ). Bone samples were fixed in 4% paraformaldehyde (Sigma) within 24 h after collection and cut parallel to the fused suture to create beams containing only parietal bone (Figure 1). Samples were wrapped in sterile gauze soaked in phosphate-buffered saline (PBS) (Gibco) and stored in sterile tubes at  $-20^{\circ}\text{C}$  until the time of the micro-computed tomography ( $\mu\text{CT}$ ) scanning.

Prior to  $\mu\text{CT}$  scanning, parietal bone samples were defrosted at room temperature and wrapped in gauze with PBS to prevent from drying during the scan. Scans were acquired using an XTH225 ST microfocuss-CT scanner (Nikon Metrology, Tring, UK) with a multimetal target. The target material used for this study was Tungsten, with 1-mm thick aluminium filter applied to reduce beam-hardening artefact. The accelerating voltage selected was 110 kV, with a current of  $64\ \mu\text{A}$  for all scans. CT scans were reconstructed

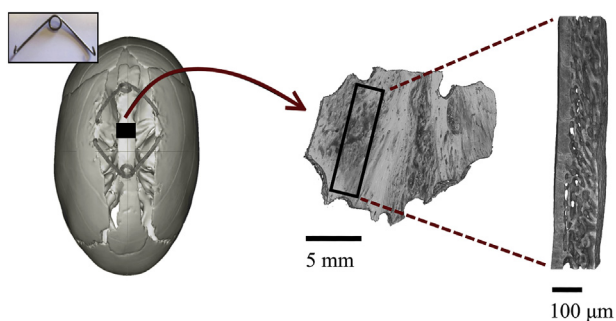


**Figure 1** Collection and micro-computed tomography scanning of parietal bone samples discarded from spring-assisted cranioplasty. The location of the collected sample, around mid-way between the anterior and posterior fontanelles, is indicated as a black rectangle on the head model; 3D representation of the whole sample, including fused sagittal suture; and the piece of parietal bone cut parallel to the fused suture, which is used for the structural analysis.

using proprietary software (CTPro3D, Nikon Metrology UK) by using modified Feldkamp filtered back projection. The resultant volumes had isotropic voxel sizes of  $5\text{--}8\ \mu\text{m}$  (equivalent to an approximate resolution of  $6\text{--}9\ \mu\text{m}$ ) depending on the degree of magnification achieved, which was limited by specimen size.

Bone structure derived from  $\mu\text{CT}$  was assessed as shown in Figure 2. First, grey value stacks of original images were used to visually classify bone into (i) one-layered cancellous bone and (ii) three-layered bone with a sandwich structure of inner and outer tables and a diploë cavity (Figure 2a). Quantitative measurement of bone structure was performed following the guidelines of Bouxsein et al.<sup>20</sup> Post-processing was carried out using the ImageJ software<sup>21</sup>: thresholding was applied to the original stacks to segment the bone matrix, which resulted in a stack of binary images with mineralised bone tissue in black (Figure 2b, 'binarised bone'); holes within the bone were filled to obtain an image representing the total cranial bone as a solid volume (Figure 2c, 'binarised total'). Bone structural parameters were measured using BoneJ plugin.<sup>22</sup> The binarised images were used to calculate bone volume (BV) and bone surface area (BS), while average thickness (Th), total volume of interest (TV) and total surface (TS) were calculated from the 'binarised total' images. Bone volume fraction (BV/TV) was computed as the percentage of bone to total volume. Bone surface density (BS/TV) was calculated as a ratio between bone surface and total volume. Because compact bone has less bone surface area than bone structured with many small trabeculae, BS/TV is higher in trabecular-like bones.

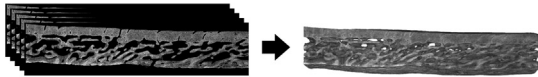
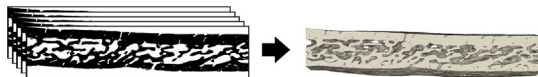

## 3D Scanning: cephalic index

Head shape change induced by SAC on the recruited patients was assessed as the difference in CI measured on 3D scans of the head acquired immediately before spring insertion ( $CI_{\text{insertion}}$ ) and immediately after their removal ( $CI_{\text{removal}}$ ) (Figure 3). Scans were acquired using a 3D handheld scanner (M4D Scanner, Rodin4D, Pessac, France) and post-processed as detailed in Tenhagen et al. (2016).<sup>23</sup> Briefly, scans were exported as 3D computational surface meshes and post-processed to clean artefacts and isolate the region of interest (i.e. the calvarium). The images were then imported to the Rhinoceros 3D software (Robert McNeel & Associates, Seattle, WA, USA) to measure cranial width and length for the computation of CI. The relative change in CI was calculated as follows [Eq. (1)]:

$$\% \text{ change in CI} = \frac{CI_{\text{removal}} - CI_{\text{insertion}}}{CI_{\text{insertion}}} \times 100 \quad (1)$$

## Statistical analysis

Statistical analysis was performed using R (v. 3.3.0, R Foundation for Statistical Computing, Vienna, Austria). Mean values and standard deviations (mean  $\pm$  SD) were calculated for the measured parameters. Normality of the data was assessed using the Shapiro–Wilk test. CIs before spring insertion ( $CI_{\text{insertion}}$ ) and after removal ( $CI_{\text{removal}}$ ) were compared using paired t-tests. Mann–Whitney–Wilcoxon

	2D stacks of images	Bone parameters
a) Original		Classification into: i) 1-layered ii) 3-layered
b) Binarized bone		Bone Volume, BV Bone Surface, BS
c) Binarized total		Thickness, Th Total Volume, TV Total Surface, TS

**Figure 2** Approach used to analyse bone structure from micro-computed tomography images. (a) 2D stacks of original images are used to visually classify bones into one- or three-layered structures. (b) Thresholding techniques are then employed to segment bone tissue and obtain binarised images with bone in black. Bone volume and surface are computed from 'binarised bone' images. (c) Holes in binarised bone images are filled to obtain the total volume of interest. Bone thickness, total volume and surface are measured on 'binarised total' images.

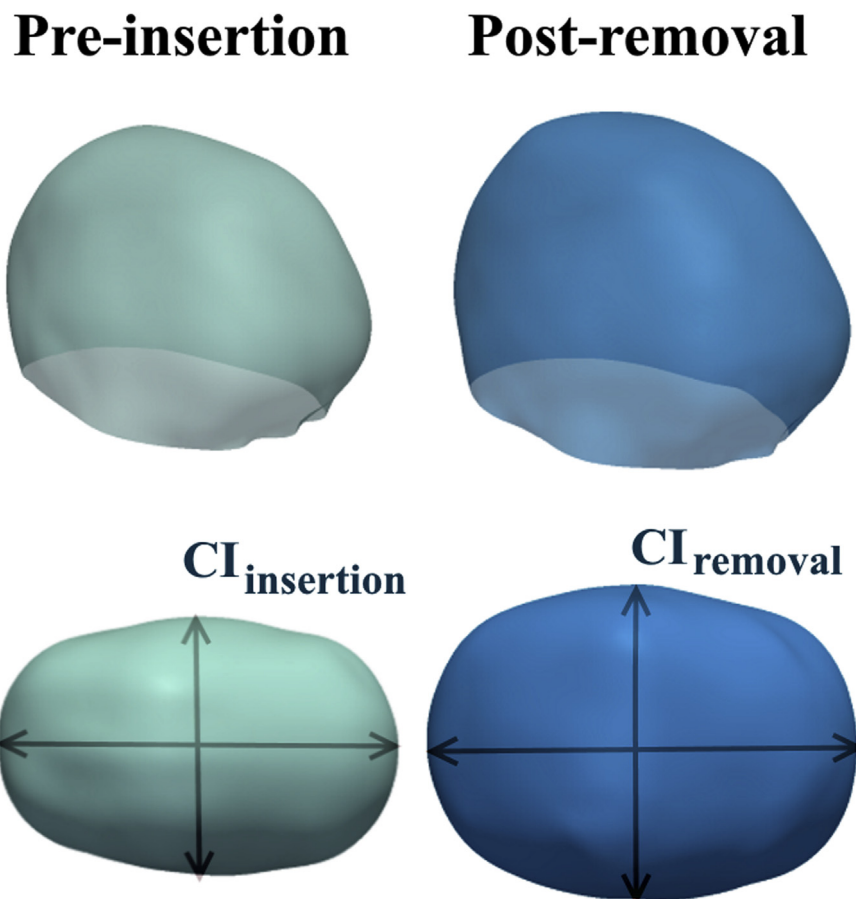


**Figure 3** 3D head scan of a patient (P10) before spring insertion (left) and after removal 4 months later (right) used to measure the cephalic index (CI).

test was used to compare the change in CI and structural parameters for one- and three-layered bones. Correlations between different parameters and changes in CI were assessed by computing Pearson's  $r$  correlation coefficient.

Cook's distance  $D^{24}$  was calculated, and data points with  $D$  greater than four times the mean were excluded from the correlation analysis. Differences were considered significant at  $p < 0.05$ .

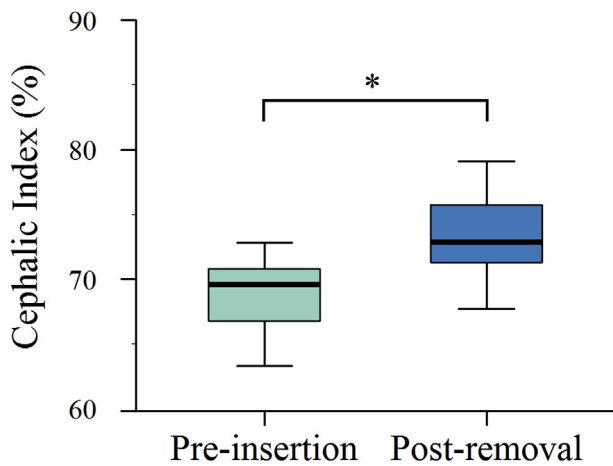


**Figure 4** Boxplots representing cephalic index (CI) of the population before spring insertion and after removal. CI is significantly higher at the time of spring removal (\* $p < 0.001$ ).

## Results

### Change in CI

CI increased from prior to spring insertion ( $CI_{\text{insertion}} = 69.0 \pm 2.7\%$ ) to post-removal ( $CI_{\text{removal}} = 73.0 \pm 3.0\%$ ) for all patients ( $p < 0.001$ ) (Figure 4). The relative increase in CI varied between 3.5% and 9.6%.

### Influence of age and treatment duration on CI

Overall, SAC resulted in bigger changes in CI for younger patients (Figure 5). However, age alone could not explain

the variation in CI improvements found in the population ( $n = 17$ , Pearson's  $r = -0.38$ ,  $p = 0.13$ ). For example, two patients of the same age had substantially different outcomes: P17 had a change in CI of 9.6%, whereas P16 had only a 4.2% change. Despite being the same age, bone structure from these two patients was different on visual assessment (Figure 5). Further, similar to age, the duration of SAC treatment from spring insertion to removal did not have a significant correlation with changes in CI ( $n = 18$ ,  $r = 0.34$ ,  $p = 0.17$ ).

## Cranial bone structure

Representative cross-sections of  $\mu$ CT scans of the collected parietal bone samples are shown in Figure 6. Eleven out of 18 bones had a one-layered structure (Figure 6a), while in seven, the two external layers of cortical bone and the diploë cavity were present (Figure 6b). The earliest time at which a diploë cavity was seen was at 4.7 months of age (P5), while the latest time at which the bone still had a one-layered structure was at 7.2 months (P17).

### Influence of cranial bone structure on CI

One-layered bones were associated with bigger changes in CI than three-layered bones ( $p = 0.016$ ) (Figure 7).

The average values of Th, BV/TV and BS/TV were  $2.37 \pm 0.59$  mm,  $50 \pm 10\%$  and  $882 \pm 143$  mm<sup>-1</sup>, respectively. There was a significant increase in Th (Figure 8a) and a decrease in BS/TV (Figure 8b) from one- to three-layered bones ( $p = 0.026$  and  $p = 0.015$ , respectively). There was no difference on BV/TV between one- and three-layered bones ( $p = 0.285$ ).

Strong relationships were found between the change in CI and average Th (Figure 9a,  $n = 18$ , Pearson's  $r = -0.79$ ,

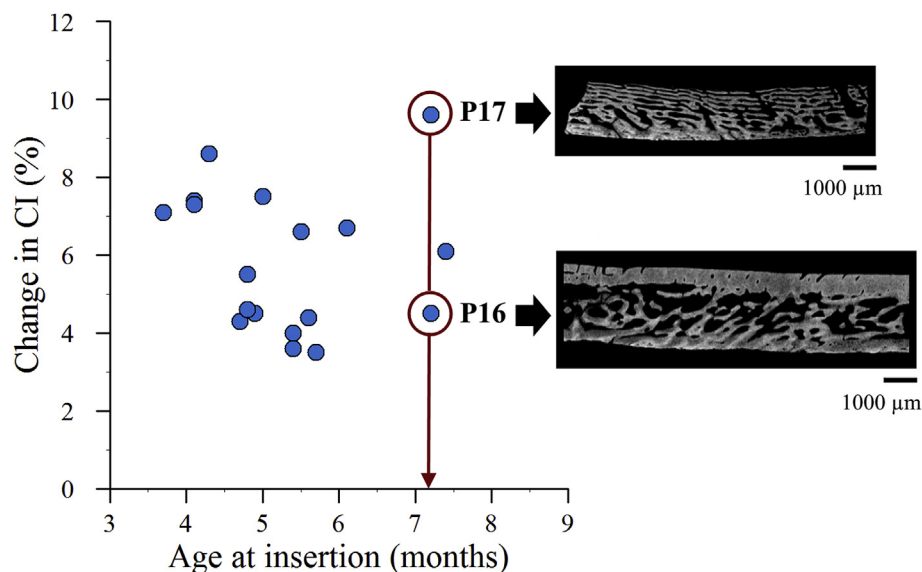


**Figure 5** Relationship between change in cephalic index (CI) and patient age at the time of spring insertion. Two 7.2-month-old patients (P16 and P17) show substantially different outcomes: P17, whose bone has a one-layered structure, shows a bigger change in CI (top) than P16 whose bone sample has a three-layered structure (bottom), as visualised through micro-computed tomography assessment.

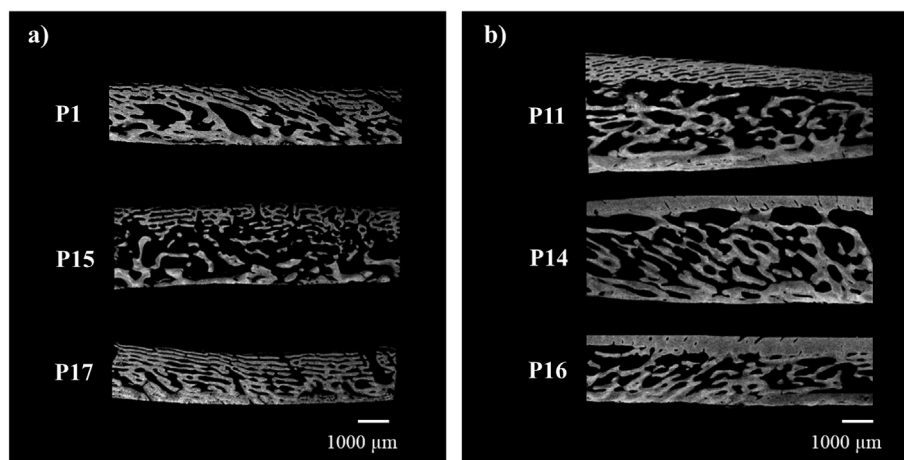


**Figure 6** Representative micro-computed tomography cross-sections of scanned parietal bones. (a) Samples with a one-layered structure from patients P1, P15 and P17; (b) Samples with a three-layered structure formed by outer cortical shells and a diploë cavity from P11, P14 and P16.

$p < 0.001$ ) and BS/TV (Figure 9b,  $n = 18$ ,  $r = 0.77$ ,  $p < 0.001$ ). No correlation was found between the change in CI and BV/TV ( $r = 0.06$ ,  $p = 0.818$ ).

## Discussion

SAC is becoming an increasingly popular surgical technique to correct scaphocephaly in children with sagittal synostosis. However, predicting head shape changes induced by the gradual opening of the springs remains challenging. This study provides insight into the relationship between cranial bone structure in children with non-syndromic single suture sagittal synostosis and surgical outcomes.

The cranial bone has a complex structure, which evolves from a one-layered cancellous tissue to a three-layered bone composed of compact inner and outer tables with a diploë cavity in the middle.<sup>14</sup> The current study revealed, through high resolution  $\mu$ CT of parietal bone samples, that in 3–8-month-old patients with sagittal synostosis, both types of structure can be distinguished. A diploë cavity was found on a patient as young as 4.7 months of age, while, some of the oldest bones still had a one-layer structure. This is of paramount importance for craniofacial surgery as the observed and quantified differences in cranial bone structure were related to the amount of change in CI achieved in SAC.

SAC induced an improvement of CI for all patients, with mean values of 69% for  $CI_{\text{insertion}}$  and 73% for  $CI_{\text{removal}}$  comparable with previous reports.<sup>3,6,23</sup> However, the relative improvement in CI was not the same for all patients. Although as a rough rule, the youngest patients yielded better results, the age of the patient alone could not explain why some older patients had bigger changes in CI than younger patients (Figure 5). In addition, increasing the duration between spring insertion and removal, which varied between 3.1 and 5.6 months, did not result in significant improvements in CI. In fact, the current study indicated that, for 3–8-month-old patients, parietal bone structure shows a stronger association with head shape changes following SAC than age or treatment duration.

The thinnest bones with the biggest BS/TV, which correspond to one-layered bones (Figure 8), led to the largest relative changes in CI (Figure 9). This suggests that one-layered bones are more susceptible for induced mechanical changes, which would be in accordance with the role that both types of parietal bones play during skull development<sup>15,18</sup>; initial one-layered bone is ‘designed’ to accommodate the growing brain, while the main function of the more mature three-layered bone is to protect the brain from external forces.

The parameter that showed the strongest correlation with changes in CI was the average bone thickness, which

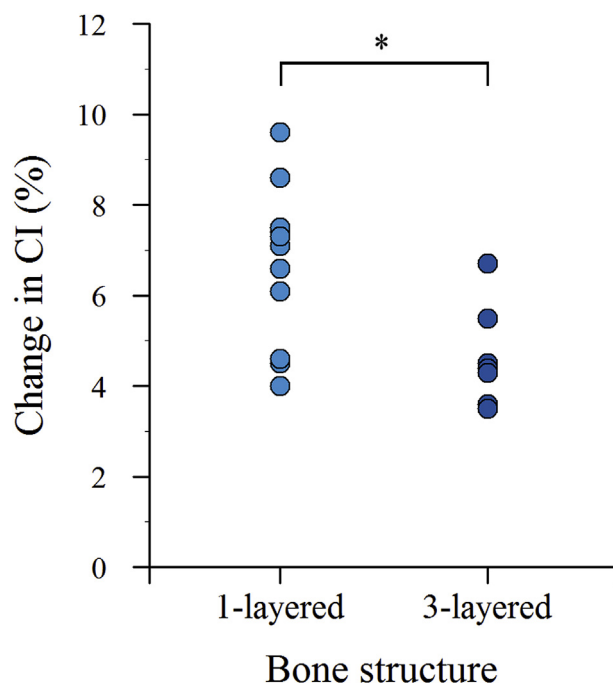


**Figure 7** Changes in cephalic index (CI) for bones classified as one or three layered. Bones with a three-layered structure display a lower change in CI. \* $p < 0.05$ .

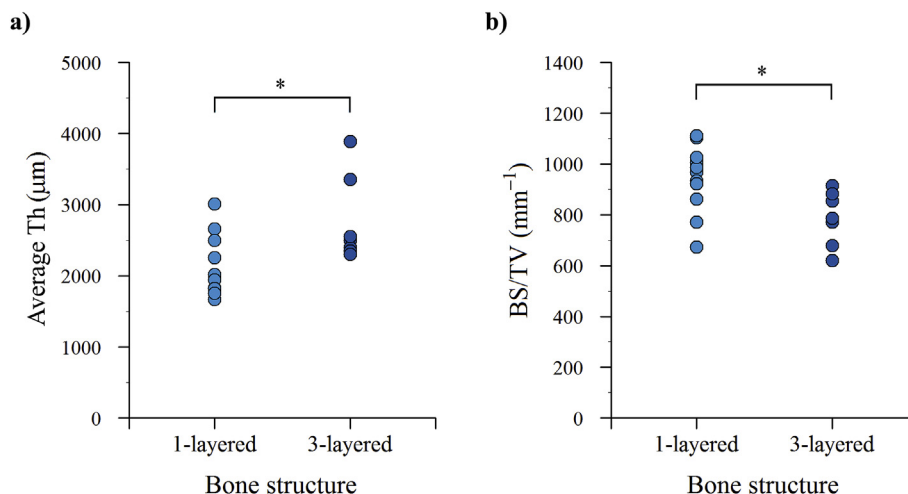


**Figure 8** Differences in (a) average thickness (Th) and (b) bone surface to total volume (BS/TV) between bones that have one- or three-layered structure. The development of the diploë cavity is associated with an increase in Th and a decrease in BS/TV. \* $p < 0.05$ .

varied between 1670 and 3800  $\mu\text{m}$ . Previous studies have measured thickness values of 1100–1800  $\mu\text{m}$ <sup>17</sup> and 3400–4100  $\mu\text{m}$ <sup>25</sup> for a similar age range in non-craniosynostotic infants by using computed tomography (CT) scans. Although our measurements are within the reported values, it is not clear how parietal thickness and structure of infants with sagittal synostosis compare to healthy controls. It must also be noted that only small parietal samples adjacent to the fused suture were analysed in this study; hence, how the structure of skull bone changes during infancy remains a question for future studies.

In summary, our results demonstrate that the effectiveness of SAC is related to the degree of development of a three-layered structure to the calvarium and bone thickness. It is also clear that the three-layered structure develops at different ages and that bone increases in

thickness at varying rates between infants. Although young patients are more likely to have one-layered bone, operating only on patients younger than 4.7 months old, which is the earliest time in which a three-layered bone was found in the current study, would leave out older patients who could have equal or even greater benefit from SAC. In our patient cohort, bone thickness proved to be a better indicator of SAC performance than age. The biggest improvements in CI were found for patients whose bones were thinner than 2 mm, while patients with bones thicker than 3 mm showed an improvement of CI of less than 4% (Figure 9). This suggests that pre-operative analysis of cranial bone thickness could be a useful adjunct in predicting surgical outcome for children undergoing SAC.  $\mu\text{CT}$  cannot obviously be used to assess patients pre-operatively; hence, some of the parameters analysed here cannot be retrieved for patients. However, cranial

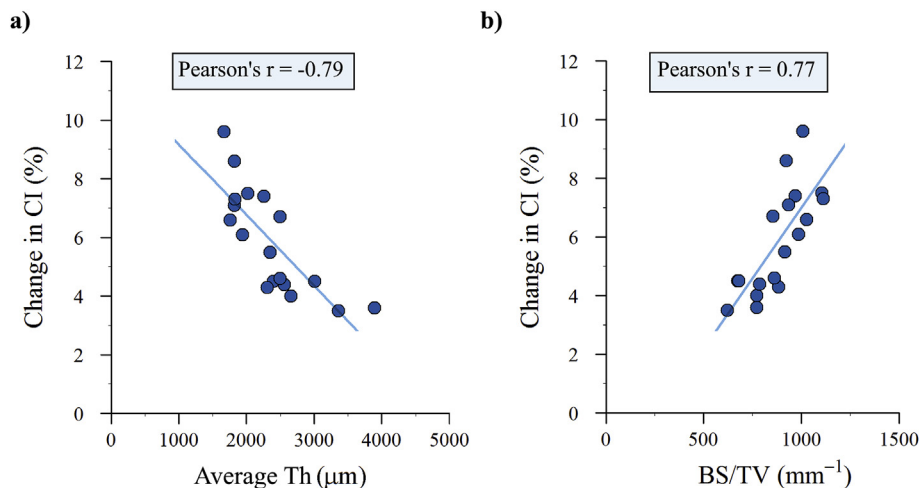


**Figure 9** Analysis of change in cephalic index (CI) following spring-assisted cranioplasty. The change in CI is strongly correlated with (a) bone average thickness (Th) and (b) bone surface to total volume (BS/TV). Both correlation coefficients are significant at  $p < 0.001$ .

thickness can be measured from CT head scans<sup>25,26</sup> or non-invasively using ultrasound techniques<sup>27–29</sup> and therefore could be used to plan surgery accordingly.

Furthermore, a deeper understanding of bone micro-structure in infants with sagittal synostosis could have implications for other craniofacial techniques<sup>26</sup> such as helmet therapy<sup>30</sup> and distraction osteogenesis,<sup>31</sup> all of which rely on the malleability of infant cranial bone to achieve desirable head shape changes—which, as shown in this study, inherently depend on the bone. Given the different surgical treatments available for the correction of sagittal synostosis,<sup>4,5,32–35</sup> future studies relating skull bone to surgical outcomes could help determine the optimal type of surgical intervention for each patient.

There are two limitations of our study. First, CI alone is a rather crude measure of surgical outcome in the treatment of sagittal synostosis, but for the purpose of the current study, we believe this measure provides insightful information for our analysis. Second, children with sagittal synostosis are a rather heterogeneous group, with different parts of the sagittal suture and indeed the calvarium being affected to varying degrees in individual children. For our study, we have analysed the micro-structure of a small rectangular piece of bone and extrapolated this to represent the structure of the calvarium. This does induce a degree of sampling error. This piece, however, is obtained from a standard location, typically half way between the site of the anterior and posterior fontanelles, and we believe is representative of the underlying pathology and structure.

## Conclusion

Scans of parietal bone samples from infants with non-syndromic sagittal synostosis undergoing SAC were acquired, for the first time, using high-resolution  $\mu$ CT. Results demonstrated that differences in bone structure strongly affected head shape changes induced by SAC, which could not be explained by patient age alone. This study suggests that pre-operative analysis of cranial bone structure can be used as a better predictor of outcome compared with the age in patients treated with SAC. Given that there are multiple proven treatment options for these kids,<sup>36</sup> we believe this is an important additional assessment when planning surgical strategies for children with sagittal synostosis to ensure SAC can provide optimal patient-specific outcomes.

## Ethical approval

Ethical approval was obtained for the collection, storage and analysis of the tissue samples (UK REC 09/H0722/28) and use of image data for research purposes (UK REC 15/LO/0386). All parents/guardians gave written informed consent to participate in this study.

## Financial disclosure statement

None of the authors has a financial interest in any of the products, devices, or drugs mentioned in this manuscript.

## Conflict of interest statement

The authors declare no conflict of interest.

## Acknowledgements and funding

The authors are grateful to Nikon Metrology for their advice regarding the acquisition and reconstruction of micro-computed tomography volumes. This research was supported by the GOSH charity through the FaceValue programme (grant no. 508847), the Engineering and Physical Sciences Research Council award (EP/N02124X/1), the Royal College of Surgeons Blond Research Training Fellowship (AI) and NIHR Clinician Scientist fellowship award (NIHR-CS-012-002) (OJA). This work was undertaken at GOSH/ICH, UCLH/UCL who received a proportion of funding from the United Kingdom Department of Health's NIHR Biomedical Research Centre funding scheme. The views expressed in this publication are those of the author(s) and not necessarily those of the NHS, Royal College of Surgeons, the NIHR or the Department of Health.

## References

1. Lauritzen CGK, Davis C, Ivarsson A, Sanger C, Hewitt TD. The evolving role of springs in craniofacial surgery: the first 100 clinical cases. *Plast Reconstr Surg* 2008;**121**(2):545–54. <http://dx.doi.org/10.1097/01.prs.0000297638.76602.de>.
2. Maltese G, Fischer S, Strandell A, Tarnow P, Kölby L. Spring-assisted surgery in the treatment of sagittal synostosis: a systematic review. *J Plast Surg Hand Surg* 2015;**49**(3):177–82. <http://dx.doi.org/10.3109/2000656X.2014.981268>.
3. van Veelen M-LC, Mathijssen IMJ. Spring-assisted correction of sagittal suture synostosis. *Childs Nerv Syst ChNS Off J Int Soc Pediatr Neurosurg* 2012;**28**(9):1347–51. <http://dx.doi.org/10.1007/s00381-012-1850-5>.
4. Arko L, Swanson JW, Fierst TM, et al. Spring-mediated sagittal craniosynostosis treatment at the Children's Hospital of Philadelphia: technical notes and literature review. *Neurosurg Focus* 2015;**38**(5):E7. <http://dx.doi.org/10.3171/2015.3.FOCUS153>.
5. Gerety PA, Basta MN, Fischer JP, Taylor JA. Operative management of nonsyndromic sagittal synostosis: a head-to-head meta-analysis of outcomes comparing 3 techniques. *J Craniofac Surg* 2015;**26**(4):1251–7. <http://dx.doi.org/10.1097/SCS.0000000000001651>.
6. David LR, Plikaitis CM, Couture D, Glazier SS, Argenta LC. Outcome analysis of our first 75 spring-assisted surgeries for scaphocephaly. *J Craniofac Surg* 2010;**21**(1):3–9. <http://dx.doi.org/10.1097/SCS.0b013e3181c3469d>.
7. Pyle J, Glazier S, Couture D, Sanger C, Gordon S, David L. Spring-assisted surgery—a surgeon's manual for the manufacture and utilization of springs in craniofacial surgery. *J Craniofac Surg* 2009;**20**(6):1962–8. <http://dx.doi.org/10.1097/SCS.0b013e3181bd2cb2>.
8. Ou Yang O, Marucci DD, Gates RJ, et al. Analysis of the cephalometric changes in the first 3 months after spring-assisted cranioplasty for scaphocephaly. *J Plast Reconstr Aesthet Surg* 2017;**70**(5):673–85.
9. Windh P, Davis C, Sanger C, Sahlin P, Lauritzen C. Spring-assisted cranioplasty vs pi-plasty for sagittal synostosis—a long term follow-up study. *J Craniofac Surg* 2008;**19**(1):59–64. <http://dx.doi.org/10.1097/scs.0b013e31815c94c8>.



10. Weiner S, Wagner HD. The material bone: structure-mechanical function relations. *Annu Rev Mater Sci* 1998;28(1):271–98. <http://dx.doi.org/10.1146/annurev.matsci.28.1.271>.
11. Currey JD. *Bones: structure and mechanics*. Princeton University Press; 2002.
12. Davis C, Windh P, Lauritzen CGK. Adaptation of the cranium to spring cranioplasty forces. *Childs Nerv Syst ChNS Off J Int Soc Pediatr Neurosurg* 2010;26(3):367–71. <http://dx.doi.org/10.1007/s00381-009-1026-0>.
13. Davis C, Windh P, Lauritzen CGK. Spring-assisted cranioplasty alters the growth vectors of adjacent cranial sutures. *Plast Reconstr Surg* 2009;123(2):470–4. <http://dx.doi.org/10.1097/PRS.0b013e3181954ce3>.
14. Davis C, Windh P, Lauritzen CGK. Cranial bone and suture strains incident to spring-assisted cranioplasty. *Plast Reconstr Surg* 2010;125(4):1104–10. <http://dx.doi.org/10.1097/PRS.0b013e3181d0abb4>.
15. Margulies SS, Thibault KL. Infant skull and suture properties: measurements and implications for mechanisms of pediatric brain injury. *J Biomech Eng* 2000;122(4):364–71.
16. Tubbs RS, Bosmia AN, Cohen-Gadol AA. The human calvaria: a review of embryology, anatomy, pathology, and molecular development. *Childs Nerv Syst* 2011;28(1):23–31. <http://dx.doi.org/10.1007/s00381-011-1637-0>.
17. Breisch E, Haas EA, Masoumi H, Chadwick AE, Krous HF. A morphometric analysis of the infant calvarium and dura. *Forensic Sci Med Pathol* 2010;6(4):249–54. <http://dx.doi.org/10.1007/s12024-009-9136-2>.
18. II. Osteology. 1. Development of the Skeleton. Gray, Henry. 1918. *Anatomy of the Human Body*. <http://www.bartleby.com/107/17.html>. [Accessed 19 August 2016].
19. Rodgers W, Glass GE, Schievano S, et al. Spring assisted cranioplasty for the correction of non-syndromic scaphocephaly: a quantitative analysis of 100 consecutive cases. *Plast Reconstr Surg* 2017 Jul;140(1):125–34. <http://dx.doi.org/10.1097/PRS.0000000000003465>.
20. Bouxsein ML, Boyd SK, Christiansen BA, Guldberg RE, Jepsen KJ, Müller R. Guidelines for assessment of bone microstructure in rodents using micro-computed tomography. *J Bone Miner Res* 2010;25(7):1468–86. <http://dx.doi.org/10.1002/jbmr.141>.
21. Schneider CA, Rasband WS, Eliceiri KW. NIH Image to ImageJ: 25 years of image analysis. *Nat Methods* 2012;9(7):671–5. <http://dx.doi.org/10.1038/nmeth.2089>.
22. Doube M, Klosowski MM, Arganda-Carreras I, et al. BoneJ: free and extensible bone image analysis in ImageJ. *Bone* 2010;47(6):1076–9. <http://dx.doi.org/10.1016/j.bone.2010.08.023>.
23. Tenhagen M, Bruse JL, Rodriguez-Florez N, et al. Three-dimensional handheld scanning to quantify head-shape changes in spring-assisted surgery for sagittal craniosynostosis. *J Craniofac Surg* 2016;27(8):2117–23. <http://dx.doi.org/10.1097/SCS.0000000000003108>.
24. Cook RD, Weisberg S. *Residuals and influence in regression*. New York: Chapman and Hall; 1982. <http://conservancy.umn.edu/handle/11299/37076>. [Accessed 26 September 2016].
25. Delye H, Clijmans T, Mommaerts MY, Sloten JV, Goffin J. Creating a normative database of age-specific 3D geometrical data, bone density, and bone thickness of the developing skull: a pilot study. *J Neurosurg Pediatr* 2015;16(6):687–702. <http://dx.doi.org/10.3171/2015.4.PEDS1493>.
26. Ghosh TD, Skolnick G, Nguyen DC, et al. Calvarial thickness and diploic space development in children with sagittal synostosis as assessed by computed tomography. *J Craniofac Surg* 2014;25(3):1050–5. <http://dx.doi.org/10.1097/SCS.0000000000000762>.
27. Elahi MM, Lessard ML, Hakim S, Watkin K, Sampalis J. Ultrasound in the assessment of cranial bone thickness. *J Craniofac Surg* 1997;8(3):213–21.
28. Federspil PA, Tretbar SH, Böhlen FH, Rohde S, Glaser S, Plinkert PK. Measurement of skull bone thickness for bone-anchored hearing aids: an experimental study comparing both a novel ultrasound system (SonoPointer) and computed tomographic scanning to mechanical measurements. *Otol Neurotol Off Publ Am Otol Soc Am Neurotol Soc Eur Acad Otol Neurotol* 2010;31(3):440–6. <http://dx.doi.org/10.1097/MAO.0b013e3181d2775f>.
29. Tretbar SH, Plinkert PK, Federspil PA. Accuracy of ultrasound measurements for skull bone thickness using coded signals. *IEEE Trans Biomed Eng* 2009;56(3):733–40. <http://dx.doi.org/10.1109/TBME.2008.2011058>.
30. Chong S, Wang K-C, Phi JH, Lee JY, Kim S-K. Minimally invasive suturectomy and postoperative helmet therapy: advantages and limitations. *J Korean Neurosurg Soc* 2016;59(3):227–32. <http://dx.doi.org/10.3340/jkns.2016.59.3.227>.
31. Munding GS, Rehim SA, Johnson O, et al. Distraction osteogenesis for surgical treatment of craniosynostosis: a systematic review. *Plast Reconstr Surg* 2016;138(3):657–69. <http://dx.doi.org/10.1097/PRS.0000000000002475>.
32. Bonfield CM, Lee PS, Adamo MA, Pollack IF. Surgical treatment of sagittal synostosis by extended strip craniectomy: cranial index, nasofrontal angle, reoperation rate, and a review of the literature. *J Cranio Maxillofac Surg* 2014;42(7):1095–101. <http://dx.doi.org/10.1016/j.jcms.2014.01.036>.
33. Taylor JA, Maugans TA. Comparison of spring-mediated cranioplasty to minimally invasive strip craniectomy and barrel staving for early treatment of sagittal craniosynostosis. *J Craniofac Surg* 2011;22(4):1225–9. <http://dx.doi.org/10.1097/SCS.0b013e31821c0f10>.
34. Thomas GPL, Johnson D, Byren JC, et al. Long-term morphological outcomes in nonsyndromic sagittal craniosynostosis: a comparison of 2 techniques. *J Craniofac Surg* 2015;26(1):19–25. <http://dx.doi.org/10.1097/SCS.0000000000001107>.
35. Fischer S, Maltese G, Tarnow P, Wikberg E, Bernhardt P, Kölby L. Comparison of intracranial volume and cephalic index after correction of sagittal synostosis with spring-assisted surgery or Pi-plasty. *J Craniofac Surg* 2016;27(2):410–3. <http://dx.doi.org/10.1097/SCS.0000000000002519>.
36. Chummun S, McLean NR, Flapper WJ, David DJ. The management of nonsyndromic, isolated sagittal synostosis. *J Craniofac Surg* 2016;27(2):299–304. <http://dx.doi.org/10.1097/SCS.0000000000002363>.